Biotin Functionalized PEGylated Poly(Amidoamine) Dendrimer conjugate for Active Targeting of Paclitaxel in Cancer

Sri Vishnu Kiran Rompicharla, Preeti Kumari, Himanshu Bhatt, Balaram Ghosh, Swati Biswas

PII: S0378-5173(18)30987-6
DOI: https://doi.org/10.1016/j.ijpharm.2018.12.069
Reference: IJP 18038

To appear in: *International Journal of Pharmaceutics*

Received Date: 22 October 2018
Revised Date: 5 December 2018
Accepted Date: 17 December 2018

Please cite this article as: S. Vishnu Kiran Rompicharla, P. Kumari, H. Bhatt, B. Ghosh, S. Biswas, Biotin Functionalized PEGylated Poly(Amidoamine) Dendrimer conjugate for Active Targeting of Paclitaxel in Cancer, *International Journal of Pharmaceutics* (2018), doi: https://doi.org/10.1016/j.ijpharm.2018.12.069

Biotin Functionalized PEGylated Poly(Amidoamine) Dendrimer conjugate for Active Targeting of Paclitaxel in Cancer

Sri Vishnu Kiran Rompicharla[1], Preeti Kumari[1], Himanshu Bhatt[1], Balaram Ghosh[1], Swati Biswas[1*]

[1] *Department of Pharmacy, Birla Institute of Technology & Science-Pilani, Hyderabad Campus, Medchal, Hyderabad, Telangana 500078, India.*

***Corresponding author:**

Swati Biswas, Ph.D.

Associate professor, Department of Pharmacy,

Birla Institute of Technology & Science-Pilani, Hyderabad Campus,

Medchal, Hyderabad, Telangana 500078, India.

Phone: +91-40-66303630,

Email ID: swati.biswas@hyderabad.bits-pilani.ac.in

Abstract

In the current study, we employed poly(amidoamine) (PAMAM) dendrimers of generation 4 (G4) to deliver paclitaxel (PTX), a poorly soluble anti-cancer agent precisely to cancer cells via its conjugation on dendrimer surface. Further, G4 PAMAM has been PEGylated (PEG) and tagged with Biotin, an essential micronutrient for cellular functions, receptors of which are overexpressed in certain cancers. The synthesized multifunctional conjugates were characterized by ^{1}H NMR and zeta potential analysis techniques. In addition, the conjugates were evaluated *in vitro* in cell monolayers and 3D spheroids of biotin receptor over-expressed A549 cell line (human non-small cell lung cancer). G4 PTX PEG-Biotin conjugate penetrated at significantly higher extent in monolayers as well as spheroids as studied by flow cytometry and confocal microscopy by visualizing the cells at varied depth. The G4 PTX PEG-Biotin conjugate demonstrated higher cytotoxicity compared to free PTX and G4 PTX PEG conjugate as assessed by MTT assay in monolayers and Presto Blue assay in detached spheroidal cells. G4 PTX PEG-Biotin demonstrated significant inhibition of growth of tumor spheroids. Therefore, the newly synthesized biotin anchored PTX-conjugated dendrimer system is promising and could be further explored for efficiently delivering PTX to biotin receptor overexpressed cancers.

Key words: PAMAM dendrimers; biotin; active targeting; cancer; paclitaxel

1. Introduction

Cancer is a leading cause of death worldwide. Chemotherapy, the first line of treatment, poses deleterious effect on the normal cells in a patient's body making it a primary obstacle to the clinical application of otherwise potent anticancer drugs (Tripodo et al., 2014). The efficacy and tolerability of anticancer agents can be increased by employing target specific drug delivery systems (DDS) that can limit the associated side effects and improve treatment prognosis (Ren et al., 2015). Several potent chemotherapeutic agents like taxols, epirubicin, platinum compounds, methotrexate, doxorubicin (DOX) etc., are clinically used for a variety of cancer treatments. However, most of the chemotherapies are conventional, and therefore, pose significant adverse effects (Abraham et al., 2005; Celik et al., 2013; Šimůnek et al., 2009; Yao et al., 2007). Therefore, DDS with targeting moieties that specifically target cancer cells could be a promising treatment strategy to overcome such shortcomings (Guo et al., 2014; Hao et al., 2015; Luo et al., 2014; Quan et al., 2014).

Nanocarriers, by virtue of their size, leaky vasculatures in tumor and poor lymphatic clearance get accumulated to the tumor microenvironment via the phenomenon, commonly known as Enhanced Permeability and Retention (EPR) effect. However, a successful cancer treatment wherein sufficient amount of drug has to reach the site of action cannot solely rely on EPR or passive targeting. Cancer cells need more micronutrients than normal cells for their proliferation and survival. As a consequence, they have overexpression of certain receptors which can be actively targeted using specific ligands (Russell-Jones et al., 2004). Different ligands, including proteins, hormones, vitamins, and growth factors which are identified by cancer cells for their active internalization, are attached to the backbone of the DDSkk (Nateghian et al., 2016). If the circulation times are long enough, effective transport to the site

of action and substantial uptake of drug via endocytosis can be possible through both - the EPR effect and active targeting of molecules (Brigger et al., 2002; Byrne et al., 2008; Chen et al., 2010).

Biotin (vitamin H) is an essential micronutrient, which is vital for normal cellular function (Livaniou et al., 2000). Owing to low molecular weight, relatively simple biochemical structure, and high tumor specificity, biotin has attracted great attention from pharmaceutical research. In order to thrive and multiply rapidly, cancer cells need extra biotin as compared to normal cells. Rapidly proliferating malignant cells overexpress biotin in order to meet their biotin uptake. Biotin overexpression is observed in wide types of cancers, including renal (RENCA, RD0995), lung (A549, M109), ovarian (OV 2008, ID8), mastocytoma (P815) and breast (4T1, JC, MMT06056) cancer cell lines (Shi et al., 2014). This specific interaction of biotin and its receptors has been explored to develop various biotin-conjugated nanocarriers to increase the uptake of anticancer drugs by various tumor cells (Bu et al., 2013; Minko et al., 2002; Taheri et al., 2011; Tseng et al., 2009; Vadlapudi et al., 2013; Yang et al., 2009; Yang et al., 2014; Yellepeddi et al., 2009).

Dendrimers are hyperbranched macromolecules having monodispersed three-dimensional structure with specific molecular weight and available in many generations based on the layer of branches put on the core (Cheng et al., 2008; Esfand and Tomalia, 2001). Poly(amidoamine) (PAMAM) dendrimers are the first commercially used class of dendrimers for drug delivery investigations (Tomalia, 2005). In general, the dendrimers possess vacant internal pockets which can hold the poorly soluble cargoes (Jansen and Meijer, 1994). Additionally, the outer shell of dendrimers possess a wide number and variety of surface functional groups which can be conjugated or anchored with various moieties (Majoros et al.,

2006; Thomas et al., 2005). PAMAM dendrimers have been widely explored for delivery of poorly soluble anti-cancer agents to specific target sites (Asthana et al., 2005; Bhadra et al., 2005; Bhadra et al., 2003; D'emanuele et al., 2004; Milhem et al., 2000; Najlah et al., 2006, 2007). Further, PAMAM dendrimers find application in gene delivery with specificity to cancer cells (Li et al., 2018; Liu et al., 2017). Ease of fabrication, nanometer size, biocompatibility, scalability are some of the advantages that make dendrimers a potential drug delivery system (Duncan and Izzo, 2005; Svenson and Tomalia, 2012). Previous studies reported the active targeting of dendrimers by conjugation of ligands such as folic acid (Thomas et al., 2005), biotin (Xu et al., 2007; Yellepeddi et al., 2009), Lactobionic acid (Iacobazzi et al., 2017), antibodies (Patri et al., 2004), peptides (Shukla et al., 2005), and epidermal growth factor (Barth et al., 2004) to dendrimers thereby enhancing the therapeutic potential of cancer chemotherapeutics.

In the present study, we have developed and investigated the potential of biotin conjugated PEGylated multifunctional PAMAM dendrimer system to effectively deliver paclitaxel (PTX), a chemotherapeutic agent which suffers poor physicochemical properties. The unique globular structure of PAMAM dendrimers allows the spatial arrangement of biotin molecules on the surface which might contribute to superior internalization of the delivery system into the cancer cells (Yellepeddi et al., 2009). Following the synthesis, we have characterized the conjugates and evaluated the delivery system in biotin overexpressed human lung cancer cell line (A549). A 3D tumor spheroid model which mimics *in vivo* tumor has been employed to evaluate the uptake and therapeutic potential of the developed dendrimer system.

2. Materials and methods

2.1 Materials

Poly(amidoamine) dendrimer of ethylenediamine core and generation 4.0 with 64 terminal amino groups (G4 PAMAM) was procured from Dendritech (USA). A gratis sample of Paclitaxel (PTX) was received from Fresenius Kabi India Pvt., Ltd. (Gurgaon, India). Methoxy-polyethyleneglycol-succinimidyl carboxymethyl ester of molecular weight 2000 Da (mPEG-SCM ester) was purchased from Jenkem Technology (USA). N-(3-Dimethylaminopropyl)-N′-ethylcarbodiimide hydrochloride (EDC. HCl, 98%), Biotin and N-Hydroxysuccinimide (NHS, 98%) were procured from Sigma Aldrich Chemicals (USA). Regenerated cellulose dialysis membrane of molecular weight cut-off 2 kDa, 3.5 kDa and 14 kDa was purchased from Spectrum Laboratories, Inc. (USA). N-ethyldiisopropylamine (DIPEA), NHS-Fluorescein was purchased from Avra Chemicals (India), and Thermo Scientific (USA) respectively. N,N'-Dicyclohexylcarbodiimide (DCC) was purchased from Spectrochem Chemicals Ltd. (India). The solvents and reagents utilized in the study were of analytical grade.

2.2 Methods

2.2.1 Synthesis of multifunctional PAMAM dendrimer

2.2.1.1 Synthesis of fluorescently tagged G4 PAMAM dendrimer

Fluorescently labelled G4 PAMAM dendrimer was prepared following an earlier reported procedure with a small modification (Biswas et al., 2012). To the DMF solution of G4 dendrimer (100 mg), Fluorescein NHS was added at a mole ratio of 1:1 dropwise under inert atmosphere. The solution was stirred in dark conditions for 8 h at normal room temperature.

Following the reaction, DMF was removed using rotary evaporator and resulting product was subjected to dialysis to remove unconjugated fluorescein. After dialyzing for 48 h, the product (F-G4) was freeze dried and stored until further use.

2.2.1.2 Synthesis of G4-PTX

The OH group at 2` position of paclitaxel (PTX) was modified to its hemisuccinate form using succinate linker (succinic anhydride) prior to reacting with amine groups of G4 PAMAM dendrimer. In brief, 25 mg of PTX was dissolved in dichloromethane and reacted with succinic anhydride (4.4 mg) for 3 days under stirring in presence of dry pyridine. The product was collected by ethyl acetate extraction and dried to yield PTX-2`-hemisuccinate as white solid. The hemisuccinate –COOH group was reacted with DCC/NHS for 8 h to form NHS ester of PTX which can easily attach with –NH2 surface groups of dendrimer molecules. The activated PTX NHS ester was added to 50 mg of G4 dendrimer in DMF at a mole ratio of 1:4 and stirred overnight. Following the reaction, DMF was evaporated and the product was dialyzed using cellulose ester membrane of MWCO 12-14 kDa against water to remove impurities. Further, a white fluffy product of G4-PTX was collected by freeze drying.

The schematic representation of synthesis of the multifunctional PAMAM dendrimer is shown in Figure 1.

2.2.1.3 Synthesis of G4-PTX-PEG

The G4-PTX construct was further attached with PEG using mPEG SCM ester (2 kDa). G4-PTX was dissolved in DMF, and mPEG SCM was added drop-wise at a mole ratio of G4-PTX: mPEG-SCM as 1:12. The reaction mixture was stirred overnight in presence of DIPEA (20 µl). The solvent was removed using rotary evaporator. The product was subjected to

dialysis using regenerated cellulose dialysis membranes of MW cutoff 12-14 kDa with frequent water changes for 48 h. After dialysis, the product was freeze dried to obtain a solid white product of G4-PTX-PEG. The fluorescently tagged dendrimer conjugates were also prepared in the same manner. The PEGylation of G4-PTX was confirmed by measuring the zeta potential changes, and by ^{1}NMR and GPC analysis.

2.2.1.4 Biotinylation of G4-PTX-PEG

Biotinylation of G4-PTX-PEG conjugate was performed by activating the carboxy group of biotin molecule using EDC/NHS (3 mol equivalent of biotin) in DMF and attaching it with amine group of G4-PTX-PEG at a mole ratio of biotin: G4-PTX-PEG as 30:1. After reaction, the solvent was removed using rotary evaporator and the product was subjected to dialysis against water for 2 days. The final G4-PTX-PEG-Biotin construct was obtained after lyophilization.

2.2.2 Characterization of multifunctional conjugate

Characterization of the PAMAM dendrimer conjugates G4-PTX, G4-PTX-PEG, and G4-PTX-PEG-Biotin was performed by ^{1}H NMR (300 MHz, Bruker, USA) and zeta potential measurements by using dynamic light scattering instrument (Nano ZS, Malvern Instruments, UK). To determine the relative molecular weights of synthesized conjugates, gel permeation chromatography (GPC) analysis was performed. Zorbax GF-250 (9.4 mm ID X 25 cm X 4-4.5 µm) size exclusion analytical column was used to run the samples in a HPLC system (Agilent 1100 series). Tris buffer (50 mM) and KCl (100 mM) was used as eluting phase in isocratic mode at a flow rate of 1 ml/min. A calibration curve was plotted with the standard molecular

weight compounds prior to analyzing the samples. Further, to determine the morphology of the conjugate G4-PTX-PEG-Biotin, TEM analysis was performed.

2.2.3 HABA/Avidin assay

Biotin attachment to the dendrimer was quantitatively estimated using HABA/Avidin assay. This assay is based on the association of the dye HABA (4'-hydroxyazobenzene-2-carboxylic acid) to avidin and the ability of biotin molecule to displace HABA in stoichiometric fractions. HABA binds to avidin to produce a yellow-orange colored complex which absorbs at 500 nm. Biotin in the sample, if present, would displace the HABA dye and cause the absorbance to decrease. As per the manufacturer's protocol, to 900 µl of HABA/Avidin reagent, 100 µl of sample containing biotin dissolved in deionized water was added. The absorbance of the test solution was recorded at 500 nm. Further, the biotinylation degree was calculated from the absorbance values obtained.

2.2.4 Cell studies

The *in vitro* evaluation of the synthesized conjugates was performed in human lung cancer cells, A549 which were procured from National Center for Cell Sciences (NCCS, Pune, India). Cells were grown in Dulbecco's minimum essential medium (DMEM) containing 10% FBS and 1% penicillin-streptomycin solution (Himedia Labs, Mumbai). During the period of study, cell cultures were maintained in an incubator operated at 37°C with 5% CO_2.

2.2.4.1 Cellular uptake by confocal microscopy

Cellular internalization of multifunctional dendrimer conjugates was studied using confocal microscopy. Briefly, A549 cells were harvested from culture flasks at 80% confluence and counted. The cells were seeded at a cell density of 50,000 cells/well onto round coverslips

placed in 12-well plates. On the day of study, cells were treated with conjugates F-G4-PEG and F-G4-PEG-Biotin (20 µg/ml) and incubated at 37 °C for 1 h and 4 h. Also, to assess the mechanism of uptake of biotin tagged dendrimer conjugates, the cells were pre-incubated with excess free biotin (300 µm for 30 min) to saturate the biotin receptors. Further, the wells containing medium with free biotin was removed and F-G4-PEG-Biotin was added to the cells. Following incubation, cells were washed three times with sterile PBS, stained with DAPI (1 µg/ml) for 5 min, washed and fixed with 4% *para*-formaldehyde for 15 min. Using a mounting medium (Fluoromount-G), the coverslips containing cells were placed on the microscopic slides. At 40 X magnification, cells were visualized under confocal microscope (Leica DMi8, Leica Microsystems, Germany), Photographs of cells were taken in FITC and DAPI fluorescence filters. The obtained data were processed using Image *J* software.

2.2.4.2 Cellular uptake by flow cytometry

To quantitatively determine the cellular association of dendrimer conjugates, flow cytometry experiments were performed in A549 cells. The 6-well microplates were seeded with A549 cells at a cell population of 0.8×10^6 cells/well and allowed to attach overnight. Similar to the confocal microscopy study, biotin receptors were saturated by pre-incubating the cells with excess of free biotin (300 µm for 30 min) which receive F-G4-PEG-Biotin treatment to observe if the cellular uptake was mediated via biotin receptors. Cells were treated for 1 h and 4 h with F-G4-PEG and F-G4-PEG-Biotin at a concentration of 20 µg/ml. After the incubation period, cells were washed with sterile fresh PBS and then trypsinized. Cells were centrifuged and the obtained cell pellet was re-dispersed in PBS before analyzing the samples by flow cytometer (Amnis, EMD Millipore, USA). Control cells did not receive any

treatment. At least 10,000 events were collected for each sample. The data was captured as geometric mean fluorescence and was calculated using the IDEAS software V6.0.

2.2.4.3 Cell viability study

The cytotoxic activity of free PTX, G4-PTX-PEG, and G4-PTX-PEG-Biotin was studied by MTT colorimetric assay. A549 cells were seeded in 96-well plates at a population of 10,000 cells/well and allowed to attach overnight. On the day of the study, cells were treated with free PTX and PTX conjugates (0-50 µg/ml) and incubated for 24 h and 48 h at 37°C. Following incubation, formulations were removed and 50 µl of MTT reagent (5 mg/ml solution) was added to each well. The plates were further incubated for another 4 h, and MTT reagent was discarded. The purple colored formazan crystals formed in the wells were dissolved by adding DMSO (150 µl) to each well. The absorbance of the wells was measured at 570 nm using a microplate reader (Spectramax™, Molecular Devices, USA) with a reference wavelength of 630 nm. Control cells did not receive any treatment containing PTX. The cytotoxicity caused due to various treatments was calculated as percentage cell viability and is represented as a bar graph against the concentration of PTX.

2.2.5 Evaluation of Biotin tagged PAMAM Dendrimer conjugates in multicellular tumor spheroids

2.2.5.1 Formation of A549spheroids

Multicellular spheroids are 3D structures which mimic the *in vivo* tumors. In the current study, A549 tumor spheroids were prepared by liquid overlay method (Perche and Torchilin, 2012; Sarisozen et al., 2014). In brief, 1.5% (w/v) agar solution was prepared in serum free DMEM medium and autoclaved. A volume of 50 µL of the agar solution was added to each

well of a 96-well plate at the bottom to prevent cell adhesion. Care should be taken so as to not let the agar solution solidify before adding to wells. For confocal microscopy study, 8-chambered glass slides were used and to each well 150 µl of agar solution were dispersed on the inner bottom.

From the culture flasks, A549 cells were detached using trypsin and cell pellet was collected by centrifugation. To each well, cells were seeded at a density of 8,000 cells. Culture plates were centrifuged at room temperature for 15 min. After centrifugation, plates are left in the incubator. The spheroid formation was constantly supervised using an inverted microscope (Leica DMi8, Leica Microsystems, Germany). For further studies, 3 – 5 days old spheroids were used.

2.2.5.2 Penetration efficiency in multicellular tumor spheroids

The internalization of targeted and non-targeted dendrimer conjugates into the spheroids was studied using confocal microscopy. F-G4-PEG-Biotin and F-G4-PEG were added to the spheroids grown in 8-well glass chamber slides and incubated for 1 and 4 h. After that, the cancer cell spheroids were gently washed with PBS and visualized by laser scanning confocal microscope (Leica DMi8, Leica Microsystems, Germany) at 10X magnification. Z-stack images were captured to see the penetration, from the surface where fluorescence is observed to the center of spheroid at every 10 µm thickness. Image *J* software was used to process the captured images.

2.2.5.3 Flow Cytometry analysis of spheroid uptake of dendrimer conjugates

Flow cytometry study was performed to quantitatively determine the uptake of targeted and non-targeted dendrimer conjugates in 3D cell spheroids. Five-day-old spheroids were

employed in the study and incubated with F-G4-PEG and F-G4-PEG-Biotin for 1 h and 4 h. After the treatment period, 10 spheroids each of every treatment were pooled up to achieve required cell population for flow cytometry analysis. The spheroids were gently washed with sterile PBS and dissociated by adding Accutase cell detachment solution. Accutase solution is used to create single cell suspensions from a clump of cells. It contains proteolytic and collagenolytic enzymes. The obtained cell suspension after Accutase treatment was centrifuged and the single cell suspension was prepared by adding PBS. Further, the samples were run using flow cytometer and atleast 10,000 events were collected for every sample. The fluorescence intensity histograms were captured in the FITC channel for each sample. A bar diagram was plotted with geometric mean fluorescence exhibited by biotin modified and unmodified dendrimer conjugates.

2.2.5.4 Growth inhibition of multicellular tumor spheroids

The inhibitory effect of PTX formulations on the growth of A549 cancer cell spheroids was studied to evaluate the potential of synthesized conjugates in delivering the drug to tumors. The cancer cell spheroids were incubated in complete media added with free PTX, G4-PTX-PEG, and G4-PTX-PEG-Biotin at a PTX concentration of 25 μg/mL. After 24 h, the growth medium with formulations was carefully discarded and fresh growth medium was added. The magnitude of spheroidal growth inhibited by dendrimer drug conjugates was visualized using inverted microscope (Leica DMi8, Leica Microsystems, Germany). Brightfield images were captured at 10X magnification. The diameter of the spheroids at regular intervals was measured and represented as a line graph.

2.2.5.5 *In vitro* cytotoxic activity in multicellular tumor spheroids

To evaluate the cytotoxic activity of targeted and non-targeted dendrimer conjugates in multicellular tumor spheroids, Presto Blue assay was performed as per the manufacturer's instructions. Presto Blue reagent is a cell permeable resazurin-based solution which turns to a red fluorescent complex upon reduction by viable cells. The fluorescence/absorbance of the sample is measured and the cell viability is calculated. On the day of study, 3-5 day old spheroids were selected and treated with free PTX, G4-PTX-PEG, and G4-PTX-PEG-Biotin at a PTX concentration of 25 µg/ml. For each treatment, 10 individual spheroids were used as a group. Following the incubation for 24 h, the medium in the wells was carefully discarded, washed with PBS and then disaggregated by adding 50 µL of Accutase solution. The cell suspension resulted by mild shaking was subjected to centrifugation to obtain cell pellet. The samples for analysis were prepared by adding 10 µl of Presto Blue reagent to the cell pellet dispersed in 90 µl of growth medium. After a brief incubation for 2 h at 37°C, the absorbance of the samples was measured at 570 nm with a reference wavelength of 600 nm.

2.2.5.6 Live/Dead cell assay in multicellular tumor spheroids

The amount of live and dead population developed as a result of various PTX treatments to A549 cell spheroids was assessed by live/dead cell assay using Calcein Blue AM reagent. In brief, dendrimer conjugates and free PTX were added to individual spheroids at a concentration of PTX equivalent to 50 µg/ml and incubated for 24 h. Following the treatment period, spheroids were washed with PBS and stained with Calcein Blue AM reagent and Propidium iodide (PI). This assay works on the principle of diffusion of Calcein Blue AM ester passively into the cells and cleaves to calcein blue in presence of cellular esterases present in viable cells. The resultant calcein blue remains inside the cytoplasm and emits

bright blue fluorescence. Further, PI dye stains the dead population. The fluorescence emitted was observed using a fluorescence microscope (Leica DMi8, Leica Microsystems, Germany) with blue and red filters. The images were processed using Image *J* software.

2.2.6 Statistical analysis

Data were represented as a mean of atleast three individual experiments with standard deviation. Student's *t*-test (GraphPad Software, Inc.; San Diego, CA) was performed to establish significance between groups. A *p* value of less than 0.05 was considered statistically significance. The representation of *, ** or ##, *** or ### corresponds to *p* values < 0.05, 0.01 and 0.001, respectively.

3. Results and Discussion

3.1 Synthesis and characterization of multifunctional dendrimer conjugate

In the NMR spectrum, the aromatic groups of PTX resulted in peaks at δ (ppm) 7-8.5 and aliphatic protons at δ (ppm) 1.3. The protons of PEG chains were observed at δ (ppm) 3.2-4.1 whereas the protons corresponding to the PAMAM dendrimer molecule were observed at δ (ppm) 1.5-3.5 as shown in figure 2A. In figure 2B, the peak at δ (ppm) 4.4 and 4.6 corresponds to the ring juncture protons of Biotin. This data confirms the successful conjugation of biotin to the dendrimer surface to form G4-PTX-PEG-Biotin. Attachment of fluorescein moiety was confirmed by the shift in absorption maxima as determined by UV-Visible spectroscopy (Figure S1).

In addition, from the GPC analysis relative mass of each conjugate was identified. From the mass value, the approximate number of molecules anchored to each dendrimer molecule was calculated. It was observed that approximately 2.76 molecules of PTX, 10.9 molecules of PEG were attached on the dendrimer surface following the synthesis procedure mentioned above (Table S1). Further, characterization by TEM analysis illustrates that the synthesized conjugate was spherical in morphology and has size in nanometer range as depicted in Figure 2C.

Furthermore, the HABA/Avidin assay revealed the degree of biotinylation of the dendrimer molecules. The number of biotin molecules attached to each dendrimer was calculated to be 20.98 (See Table S1). Also, a variation in the zeta potential as presented in Table 1 following each synthetic step supports the successful construction of the conjugates.

3.2 Cell Studies

3.2.1 Cellular uptake by confocal microscopy

The cellular internalization of F-G4-PEG and F-G4-PEG-Biotin by the A549 cells after 1 h and 4 h treatment was observed by confocal microscopy. A bright green fluorescence was noticed in the cells treated with biotin anchored dendrimer conjugate in comparison to the cells treated with the non-targeted conjugate. The green fluorescence caused by F-G4-PEG-Biotin in cells saturated with free biotin was seen to be less in intensity than the cells without excess biotin. This suggests that the biotin targeted dendrimers internalize actively by the biotin receptors present in higher concentration on the surface of the A549 cells. The less significant uptake occurring in the presence of free biotin also suggests that the dendrimer conjugates underwent charge based adsorptive endocytosis. The adsorptive endocytosis of positively charged moieties and the biotin receptor mediated uptake together significantly improved the cellular association of the synthesized dendrimer conjugates. Further, the results of confocal microscopy corroborated with the flow cytometry analysis indicating a higher cellular uptake in cells which received F-G4-PEG-Biotin treatment compared to F-G4-PEG, in a time dependent manner. The images captured at 1 h and 4 h incubation were represented in Figure 3.

3.2.2 Cellular uptake by flow cytometry

Quantitative assessment of cellular association was performed using flow cytometry. Similar to the microscopy studies, influence of free biotin on the uptake of targeted dendrimers was also studied. The saturation of the biotin vitamin transporters with addition of excess free biotin resulted in decreased intensity of the fluorescence in the cells treated with F-G4-PEG-

Biotin. Flow cytometry data revealed a time dependent increase in the internalization at the end of 1 h and 4 h treatment. An increase in the geometric mean fluorescence was observed with time resulting in 1.53 fold and 1.94 fold higher uptake at 1 h and 4 h respectively for biotin tagged dendrimer conjugate. The results also indicated that the Biotin tagged dendrimer conjugates were promptly internalized via the biotin receptors. The role of biotin receptors in uptake of actively targeted dendrimer conjugates was understood and the data was in accordance with the confocal microscopy results. A bar graph of geometric mean fluorescence was plotted from the values obtained at 1 h and 4 h and represented along with the histograms of events collected by flow cytometer in Figure 4.

3.2.3 Cytotoxicity Study

The cytotoxicity exhibited by the dendrimer-drug conjugates compared to free drug in A549 cells was studied by MTT assay. For the experiment, cells were treated with free PTX, G4-PTX-PEG, and G4-PTX-PEG-Biotin at a concentration range of 0-50 μg/ml and placed the well plates in incubator for 24 and 48 h. From the MTT assay, it was observed that there was an overall decrease in the cell viability with increase in treatment time and concentration of the drug given to the cells (Figure 5). Of all the treatments, G4-PTX-PEG-Biotin was found to be more active in killing the cells compared to other treatments. After 24 h, cells treated with G4-PTX-PEG-Biotin exhibited 32.7±5.14% cell viability against 51.62±3.9% for G4-PTX-PEG and 62.3±3% for free PTX, respectively. Furthermore, the cell viability declined to 14.5±3.44%, 29.8±3.2%, and 43.2±2.8% for G4-PTX-PEG-Biotin, G4-PTX-PEG, and free PTX, respectively after 48 h. Dendrimer-drug conjugates were more active at all the time points compared to free PTX. Moreover, G4-PTX-PEG-Biotin had shown superior cell killing which can be ascribed to its capability of internalizing actively into the cells via the biotin

receptors which in turn delivers greater concentrations of PTX to cancer cells than non-targeted dendrimer or free drug. The uptake of the dendrimer conjugates by receptor mediated/adsorptive endocytosis could avoid the drug efflux by P-glycoprotein. A reason for lesser cytotoxicity noticed in free PTX treated cells could be due to the drug being pushed out of the cell by P-glycoprotein transporter system.

3.3 Evaluation of Biotin tagged PAMAM Dendrimer conjugates in multicellular tumor spheroids

3.3.1 Penetration efficiency in multicellular tumor spheroids

Multicellular tumor spheroidal models simulate the *in vivo* tumors in terms of tumor structure and microenvironment. 3D spheroids retain cancer cells in a natural morphology in presence of extracellular matrix, pH and oxygen gradients resembling actual tumors. Also, spheroid models mimic drug resistance in solid tumors to a greater extent compared to 2D monolayer cell system. (van den Brand et al., 2017; Yang et al., 2017). These features make 3D spheroidal cancer cell model an attractive alternative to understand the movement of molecules into the cancer tissue.

From the Z-stack images captured using confocal microscopy, it was observed that the fluorescence was deeper in spheroids treated with biotin tagged dendrimers in comparison to the non-targeted conjugate. Further, the conjugates moved into the core of the spheroids as evidenced by the bright green fluorescence at depths with increase in the time of incubation from 1 h to 4 h (Figure 6). Biotin receptor mediated uptake of F-G4-PEG-Biotin resulted in superior diffusion of dendrimer conjugates into the 3D tumor spheroids compared to non-

targeted dendrimers. This observation ascertains the advantage of active targeting to tumors by biotinylation of the delivery systems.

3.3.2 Uptake of dendrimer conjugates in multicellular spheroids by flow cytometry

The internalization of biotin targeted and non-targeted dendrimers in the 3D multicellular cancer spheroids was quantified by flow cytometry. The fluorescence intensity was observed to be higher with F-G4-PEG-Biotin conjugate treatment compared to F-G4-PEG. The biotin tagged dendrimer conjugate exhibited a 1.63 fold and 1.7-fold higher geo mean fluorescence value compared to non-targeted dendrimer conjugate following 1 h and 4 h of incubation, respectively.

The flow cytometry data supports the confocal microscopy results, where time-dependent intensification of the green fluorescence due to accumulation in the spheroids was seen. It can be affirmed that the biotin conjugation on the surface remarkably improved the uptake of the dendrimer conjugates. Data collected from flow cytometer was represented in Figure 7 as fluorescence intensity histogram and a bar graph.

3.3.3 Growth inhibition of multicellular tumor spheroids

Growth inhibition caused due to exposure of multicellular cancer spheroids to free PTX, G4-PTX-PEG, and G4-PTX-PEG-Biotin was evaluated by measuring the diameter of the tumor spheroids over a period of time. The spheroids were examined for 6 days and the microscopic images were captured on Day 0, Day 3, and Day 6 using brightfield microscope. The diameter of the spheroids was noted down to analyze their growth. As depicted in Figure 8A, the diameter of the spheroids was significantly less on treatment with PAMAM dendrimer-drug conjugates compared to free drug. Moreover, the diameter of control spheroids increased

drastically up to 1000 µm diameter during the study. In the treatment groups, the average diameter of spheroids at the end of 6 days was measured to be 531.3 ± 13.5 µm, 647 ± 32.6 µm, 791.6 ± 38.2 µm, and 927.3 ± 10 µm for G4-PTX-PEG-Biotin, G4-PTX-PEG, free PTX, and complete media (control), respectively. The plot of diameters of spheroids is illustrated as a line graph in Figure 8B.

The observation can be explained based on the cellular association data where active targeting via biotin receptors promoted the delivery system to internalize efficiently in-turn leading to localization of PTX in the spheroids obstructing their growth. This was supported by the uptake studies performed in the 3D spheroid model, where the Biotin-dendrimer conjugate significantly internalized into the spheroids, making more amount of drug available for therapeutic action at the target location. Since 3D spheroid model mimics *in vivo* solid tumors to a great extent, it could be extrapolated that the Biotin anchored PAMAM dendrimers could significantly reduce the tumor growth *in vivo*.

3.3.4 *In vitro* cytotoxic activity in multicellular tumor spheroids

The reducibility of Presto Blue reagent upon treatment with PTX formulations was used as a measure to quantify the cytotoxic activity exhibited by the formulations in the A549 multicellular spheroids. Treatment of spheroids with G4-PTX-PEG-Biotin and G4-PTX-PEG exhibited superior cytotoxicity over free drug after incubation for 24 h at all the tested concentrations. Highest degree of cytotoxicity was observed with G4-PTX-PEG-Biotin with a cell viability of 39.35 ± 2.6% whereas, G4-PTX-PEG and free PTX displayed 50.5 ± 3.7% and 68.9 ± 1.48% viability respectively (Figure 9). The cytotoxic activity in spheroids was slightly reduced in comparison to cell monolayers as the penetration of the delivery system

becomes difficult due to structural complexity than the monolayers. The efficiency of biotin tagged dendrimers to enter the cells actively promoted in superior buildup of PTX in cells to exhibit therapeutic action.

3.3.5 Live/Dead cell assay in multicellular tumor spheroids

The calcein blue AM following internalization by living cells yields emits a strong blue fluorescence due to cleavage of the ester by the intracellular esterases. The dead cells lack the ability to convert the calcein blue AM reagent yielding no fluorescence. Further, dead population in the spheroids was located in red color due to Propidium iodide staining.

From the fluorescence images of the spheroids (Figure 10), highest extent of dead population seen as bright red fluorescence was induced by biotin anchored dendrimer followed by non-targeted conjugate and free PTX. No significant dead population was observed in control spheroids.

In free PTX treated spheroids, dead cells were majorly observed towards the boundary suggesting limited penetration of free drug deeper into the spheroid mass. On the other hand, dead cell population was observed clearly on both the boundary and within the central regions of spheroid with G4-PTX-PEG and G4-PTX-PEG-Biotin treated spheroids. The study indicated active targeting and as a result of that, higher penetration of biotin modified conjugate in tumor spheroids compared to unmodified conjugate.

4. Conclusion

In this study, we have developed a G4 PAMAM dendrimer system to deliver paclitaxel (PTX) specifically to the cancer cells by following active-targeting approach. Biotin was anchored on to the surface of the dendrimers to target the vitamin uptake receptors overexpressed on the cancer cells. PTX was covalently linked to the surface of the G4 PAMAM dendrimer using a succinate linker. Further, to avoid the toxicity of dendrimers due to their cationic nature and to prolong the systemic circulation of the conjugate, PEG has been attached. The presence of biotin on the dendrimer surface was quantified using HABA/Avidin assay. G4-PTX, G4-PTX-PEG and G4-PTX-PEG-Biotin had attachments of approximately 2.76 molecules of PTX, 10.9 molecules of PEG and 20.98 molecules of biotin per molecule of G4 PAMAM dendrimer as indicated by GPC analysis of G4-PTX, and G4-PTX-PEG and HABA assay for G4-PTX-PEG-Biotin. TEM analysis revealed a spherical morphology and nanometer size range of the conjugates. Cytotoxicity study by MTT assay and, cellular uptake studies performed on A549 cells revealed that dendrimer–drug conjugates were efficient in cellular internalization and cell killing activity. Biotin saturation studies demonstrated the role of biotin receptor in mediating cellular uptake. Further, in 3D cancer cell spheroids, biotin tagged conjugate displayed superior penetration, cytotoxicity, and inhibition of growth in comparison to the treatment with non-targeted conjugate and free drug. Considering the results, it can be affirmed that the newly developed active targeted dendrimer system could be a promising treatment strategy for solid tumors and warrants further exploration for clinical translation.

Conflicts of Interest

Authors declare no conflicts of interest

Acknowledgements

This work was supported principally by the Department of Biotechnology (Bio-CARe scheme, BT/BioCARe/07/10003/2013-2014) to author Swati Biswas.

References

Abraham, S.A., Waterhouse, D.N., Mayer, L.D., Cullis, P.R., Madden, T.D., Bally, M.B., 2005. The liposomal formulation of doxorubicin, Methods Enzymol. Elsevier, pp. 71-97.

Asthana, A., Chauhan, A.S., Diwan, P.V., Jain, N.K., 2005. Poly (amidoamine)(PAMAM) dendritic nanostructures for controlled sitespecific delivery of acidic anti-inflammatory active ingredient. AAPS PharmSciTech 6, E536-E542.

Barth, R.F., Wu, G., Yang, W., Binns, P.J., Riley, K.J., Patel, H., Coderre, J.A., Tjarks, W., Bandyopadhyaya, A., Thirumamagal, B., 2004. Neutron capture therapy of epidermal growth factor (+) gliomas using boronated cetuximab (IMC-C225) as a delivery agent. Appl. Radiat. Isot. 61, 899-903.

Bhadra, D., Bhadra, S., Jain, N., 2005. Pegylated lysine based copolymeric dendritic micelles for solubilization and delivery of artemether. J. Pharm. Pharm. Sci. 8, 467-482.

Bhadra, D., Bhadra, S., Jain, S., Jain, N., 2003. A PEGylated dendritic nanoparticulate carrier of fluorouracil. Int. J. Pharm. 257, 111-124.

Biswas, S., Dodwadkar, N.S., Piroyan, A., Torchilin, V.P., 2012. Surface conjugation of triphenylphosphonium to target poly(amidoamine) dendrimers to mitochondria. Biomaterials 33, 4773-4782.

Brigger, I., Dubernet, C., Couvreur, P., 2002. Nanoparticles in cancer therapy and diagnosis. Adv. Drug Deliv. Rev. 54, 631-651.

Bu, L., Gan, L.-C., Guo, X.-Q., Chen, F.-Z., Song, Q., Gou, X.-J., Hou, S.-X., Yao, Q., 2013. Trans-resveratrol loaded chitosan nanoparticles modified with biotin and avidin to target hepatic carcinoma. Int. J. Pharm. 452, 355-362.

Byrne, J.D., Betancourt, T., Brannon-Peppas, L., 2008. Active targeting schemes for nanoparticle systems in cancer therapeutics. Adv. Drug Deliv. Rev. 60, 1615-1626.

Celik, F., Gocmez, C., Bozkurt, M., Kaplan, I., Kamasak, K., Akil, E., Dogan, E., Guzel, A., Uzar, E., 2013. Neuroprotective effects of carvacrol and pomegranate against methotrexate-induced toxicity in rats. Eur. Rev. Med. Pharmacol. Sci. 17, 2988-2993.

Chen, S., Zhao, X., Chen, J., Chen, J., Kuznetsova, L., Wong, S.S., Ojima, I., 2010. Mechanism-Based Tumor-Targeting Drug Delivery System. Validation of Efficient Vitamin Receptor-Mediated Endocytosis and Drug Release. Bioconjug. Chem. 21, 979-987.

Cheng, Y., Xu, Z., Ma, M., Xu, T., 2008. Dendrimers as drug carriers: applications in different routes of drug administration. J. Pharm. Sci. 97, 123-143.

D'emanuele, A., Jevprasesphant, R., Penny, J., Attwood, D., 2004. The use of a dendrimer-propranolol prodrug to bypass efflux transporters and enhance oral bioavailability. J. Control. Release 95, 447-453.

Duncan, R., Izzo, L., 2005. Dendrimer biocompatibility and toxicity. Adv. Drug Deliv. Rev. 57, 2215-2237.

Esfand, R., Tomalia, D.A., 2001. Poly (amidoamine)(PAMAM) dendrimers: from biomimicry to drug delivery and biomedical applications. Drug Discov. Today 6, 427-436.

Guo, H., Zhang, D., Li, T., Li, C., Guo, Y., Liu, G., Hao, L., Shen, J., Qi, L., Liu, X., 2014. In vitro and in vivo study of Gal-OS self-assembled nanoparticles for liver-targeting delivery of doxorubicin. J. Pharm. Sci. 103, 987-993.

Hao, M., Song, F., Du, X., Wang, G., Yang, Y., Chen, K., Yang, J., 2015. Advances in targeted therapy for unresectable melanoma: new drugs and combinations. Cancer letters 359, 1-8.

Iacobazzi, R.M., Porcelli, L., Lopedota, A.A., Laquintana, V., Lopalco, A., Cutrignelli, A., Altamura, E., Di Fonte, R., Azzariti, A., Franco, M., Denora, N., 2017. Targeting human liver cancer cells with lactobionic acid-G(4)-PAMAM-FITC sorafenib loaded dendrimers. Int. J. Pharm. 528, 485-497.

Jansen, J.F., Meijer, E., 1994. Encapsulation of guest molecules into a dendritic box. Science 266, 1226-1229.

Li, J., Liang, H., Liu, J., Wang, Z., 2018. Poly (amidoamine) (PAMAM) dendrimer mediated delivery of drug and pDNA/siRNA for cancer therapy. Int. J. Pharm. 546, 215-225.

Liu, J., Li, J., Liu, N., Guo, N., Gao, C., Hao, Y., Chen, L., Zhang, X., 2017. In vitro studies of phospholipid-modified PAMAM-siMDR1 complexes for the reversal of multidrug resistance in human breast cancer cells. Int. J. Pharm. 530, 291-299.

Livaniou, E., Costopoulou, D., Vassiliadou, I., Leondiadis, L., Nyalala, J.O., Ithakissios, D.S., Evangelatos, G.P., 2000. Analytical techniques for determining biotin. J. Chromatogr. A 881, 331-343.

Luo, Z., Hu, Y., Cai, K., Ding, X., Zhang, Q., Li, M., Ma, X., Zhang, B., Zeng, Y., Li, P., 2014. Intracellular redox-activated anticancer drug delivery by functionalized hollow mesoporous silica nanoreservoirs with tumor specificity. Biomaterials 35, 7951-7962.

Majoros, I.J., Myc, A., Thomas, T., Mehta, C.B., Baker, J.R., 2006. PAMAM dendrimer-based multifunctional conjugate for cancer therapy: synthesis, characterization, and functionality. Biomacromolecules 7, 572-579.

Milhem, O., Myles, C., McKeown, N., Attwood, D., D'Emanuele, A., 2000. Polyamidoamine Starburst® dendrimers as solubility enhancers. Int. J. Pharm. 197, 239-241.

Minko, T., Paranjpe, P.V., Qiu, B., Lalloo, A., Won, R., Stein, S., Sinko, P.J., 2002. Enhancing the anticancer efficacy of camptothecin using biotinylated poly (ethyleneglycol) conjugates in sensitive and multidrug-resistant human ovarian carcinoma cells. Cancer Chemother. Pharmacol. 50, 143-150.

Najlah, M., Freeman, S., Attwood, D., D'Emanuele, A., 2006. Synthesis, characterization and stability of dendrimer prodrugs. Int. J. Pharm. 308, 175-182.

Najlah, M., Freeman, S., Attwood, D., D'Emanuele, A., 2007. In vitro evaluation of dendrimer prodrugs for oral drug delivery. Int. J. Pharm. 336, 183-190.

Nateghian, N., Goodarzi, N., Amini, M., Atyabi, F., Khorramizadeh, M.R., Dinarvand, R., 2016. Biotin/folate-decorated human serum albumin nanoparticles of docetaxel: comparison of chemically conjugated nanostructures and physically loaded nanoparticles for targeting of breast cancer. Chem. Biol. Drug Des. 87, 69-82.

Patri, A.K., Myc, A., Beals, J., Thomas, T.P., Bander, N.H., Baker, J.R., 2004. Synthesis and in vitro testing of J591 antibody− dendrimer conjugates for targeted prostate cancer therapy. Bioconjug. Chem. 15, 1174-1181.

Perche, F., Torchilin, V.P., 2012. Cancer cell spheroids as a model to evaluate chemotherapy protocols. Cancer Biol. Ther. 13, 1205-1213.

Quan, Y.H., Kim, B., Park, J.-H., Choi, Y., Choi, Y.H., Kim, H.K., 2014. Highly sensitive and selective anticancer effect by conjugated HA-cisplatin in non-small cell lung cancer overexpressed with CD44. Exp. Lung Res. 40, 475-484.

Ren, W.X., Han, J., Uhm, S., Jang, Y.J., Kang, C., Kim, J.-H., Kim, J.S., 2015. Recent development of biotin conjugation in biological imaging, sensing, and target delivery. Chem. Commun. 51, 10403-10418.

Russell-Jones, G., McTavish, K., McEwan, J., Rice, J., Nowotnik, D., 2004. Vitamin-mediated targeting as a potential mechanism to increase drug uptake by tumours. J. Inorg. Biochem. 98, 1625-1633.

Sarisozen, C., Abouzeid, A.H., Torchilin, V.P., 2014. The effect of co-delivery of paclitaxel and curcumin by transferrin-targeted PEG-PE-based mixed micelles on resistant ovarian cancer in 3-D spheroids and in vivo tumors. Eur. J. Pharm. Biopharm. 88, 539-550.

Shi, J.-F., Wu, P., Jiang, Z.-H., Wei, X.-Y., 2014. Synthesis and tumor cell growth inhibitory activity of biotinylated annonaceous acetogenins. Eur. J. Med. Chem. 71, 219-228.

Shukla, R., Thomas, T.P., Peters, J., Kotlyar, A., Myc, A., Baker Jr, J.R., 2005. Tumor angiogenic vasculature targeting with PAMAM dendrimer–RGD conjugates. Chem. Commun., 5739-5741.

Šimůnek, T., Štěrba, M., Popelová, O., Adamcová, M., Hrdina, R., Geršl, V., 2009. Anthracycline-induced cardiotoxicity: overview of studies examining the roles of oxidative stress and free cellular iron. Pharmacol. Rep. 61, 154-171.

Svenson, S., Tomalia, D.A., 2012. Dendrimers in biomedical applications—reflections on the field. Adv. Drug Deliv. Rev. 64, 102-115.

Taheri, A., Dinarvand, R., Nouri, F.S., Khorramizadeh, M.R., Borougeni, A.T., Mansoori, P., Atyabi, F., 2011. Use of biotin targeted methotrexate–human serum albumin conjugated nanoparticles to enhance methotrexate antitumor efficacy. Int J Nanomedicine 6, 1863.

Thomas, T.P., Majoros, I.J., Kotlyar, A., Kukowska-Latallo, J.F., Bielinska, A., Myc, A., Baker, J.R., 2005. Targeting and inhibition of cell growth by an engineered dendritic nanodevice. J. Med. Chem. 48, 3729-3735.

Tomalia, D.A., 2005. Birth of a new macromolecular architecture: dendrimers as quantized building blocks for nanoscale synthetic polymer chemistry. Progress in Polymer Science 30, 294-324.

Tripodo, G., Mandracchia, D., Collina, S., Rui, M., Rossi, D., 2014. New perspectives in cancer therapy: the biotin-antitumor molecule conjugates. Med. Chem. 8, 1-4.

Tseng, C.-L., Su, W.-Y., Yen, K.-C., Yang, K.-C., Lin, F.-H., 2009. The use of biotinylated-EGF-modified gelatin nanoparticle carrier to enhance cisplatin accumulation in cancerous lungs via inhalation. Biomaterials 30, 3476-3485.

Vadlapudi, A.D., Vadlapatla, R.K., Pal, D., Mitra, A.K., 2013. Biotin uptake by T47D breast cancer cells: functional and molecular evidence of sodium-dependent multivitamin transporter (SMVT). Int. J. Pharm. 441, 535-543.

van den Brand, D., Massuger, L.F., Brock, R., Verdurmen, W.P., 2017. Mimicking Tumors: Toward More Predictive In Vitro Models for Peptide- and Protein-Conjugated Drugs. Bioconjug. Chem. 28, 846-856.

Xu, H., Regino, C.A., Koyama, Y., Hama, Y., Gunn, A.J., Bernardo, M., Kobayashi, H., Choyke, P.L., Brechbiel, M.W., 2007. Preparation and preliminary evaluation of a biotin-targeted, lectin-targeted dendrimer-based probe for dual-modality magnetic resonance and fluorescence imaging. Bioconjug. Chem. 18, 1474-1482.

Yang, W., Cheng, Y., Xu, T., Wang, X., Wen, L.-p., 2009. Targeting cancer cells with biotin–dendrimer conjugates. Eur. J. Med. Chem. 44, 862-868.

Yang, W., Wang, M., Ma, L., Li, H., Huang, L., 2014. Synthesis and characterization of biotin modified cholesteryl pullulan as a novel anticancer drug carrier. Carbohydr. Polym. 99, 720-727.

Yang, Y., Roy, A., Zhao, Y., Undzys, E., Li, S.-D., 2017. Comparison of Tumor Penetration of Podophyllotoxin–Carboxymethylcellulose Conjugates with Various Chemical Compositions in Tumor Spheroid Culture and In Vivo Solid Tumor. Bioconjug. Chem. 28, 1505-1518.

Yao, X., Panichpisal, K., Kurtzman, N., Nugent, K., 2007. Cisplatin nephrotoxicity: a review. Am. J. Med. Sci. 334, 115-124.

Yellepeddi, V.K., Kumar, A., Palakurthi, S., 2009. Biotinylated poly (amido) amine (PAMAM) dendrimers as carriers for drug delivery to ovarian cancer cells in vitro. Anticancer Res. 29, 2933-2943.

List of Tables

Table 1 Zeta potential values of dendrimer conjugates after each step of synthesis (Mean±SD, n=3).

Dendrimer conjugate	Zeta potential (mV)
G4	+18.1±2.2
G4-PTX	+13.3±1.8
G4-PTX-PEG	+6.3±1.26
G4-PTX-PEG-Biotin	+4.8±1.35

List of Figures

Figure 9 Live/dead cell micrographs of tumor spheroids captured using fluorescence microscope at 10X magnification. Red fluorescence (PI) depicts dead population and blue fluorescence (calcein blue) depicts live population.

Figure 1:

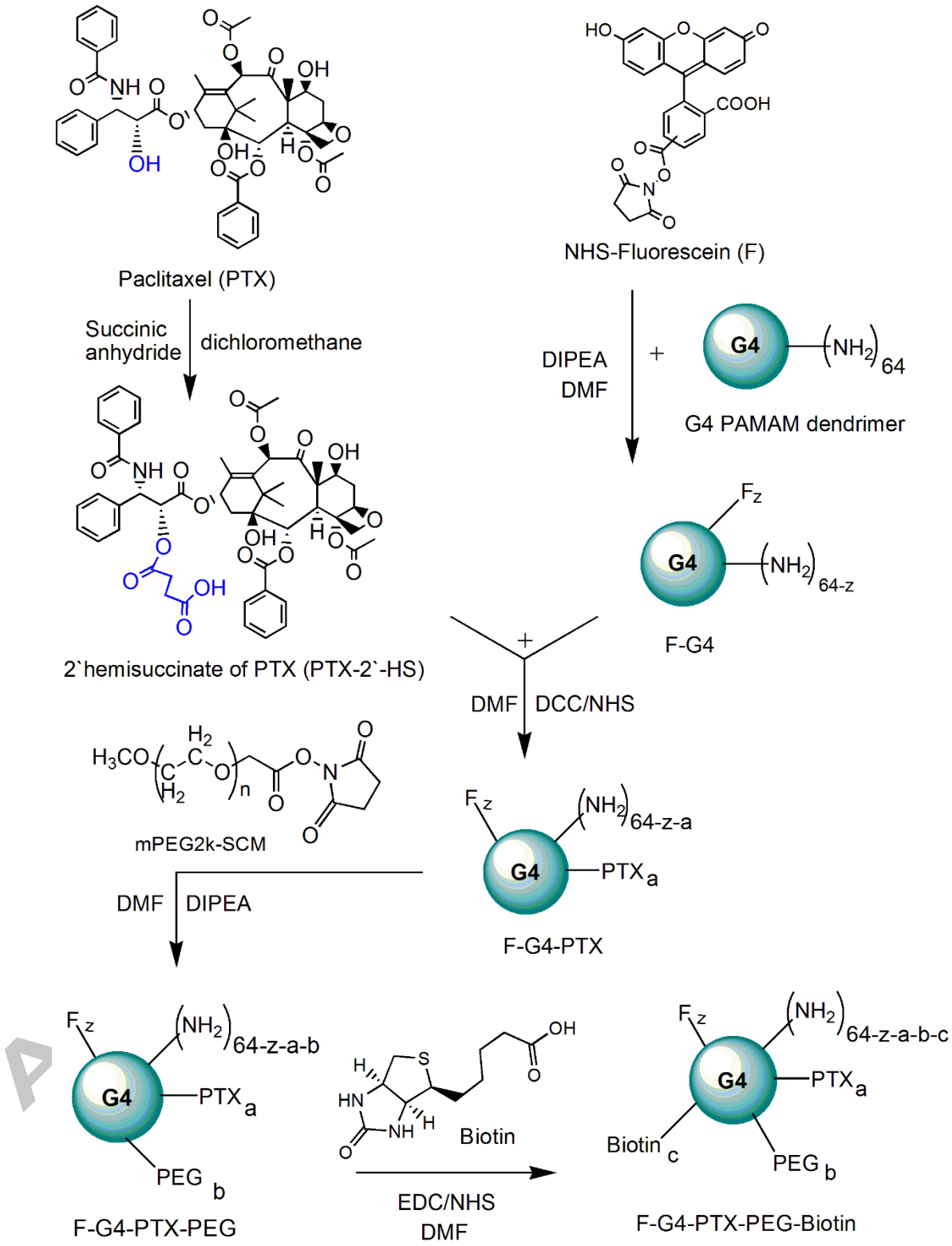
Paclitaxel (PTX)
NHS-Fluorescein (F)
Succinic anhydride
dichloromethane
DIPEA
DMF
G4 PAMAM dendrimer
2`hemisuccinate of PTX (PTX-2`-HS)
F-G4
DMF
DCC/NHS
mPEG2k-SCM
DMF
DIPEA
F-G4-PTX
F-G4-PTX-PEG
Biotin
EDC/NHS
DMF
F-G4-PTX-PEG-Biotin

Figure 2:

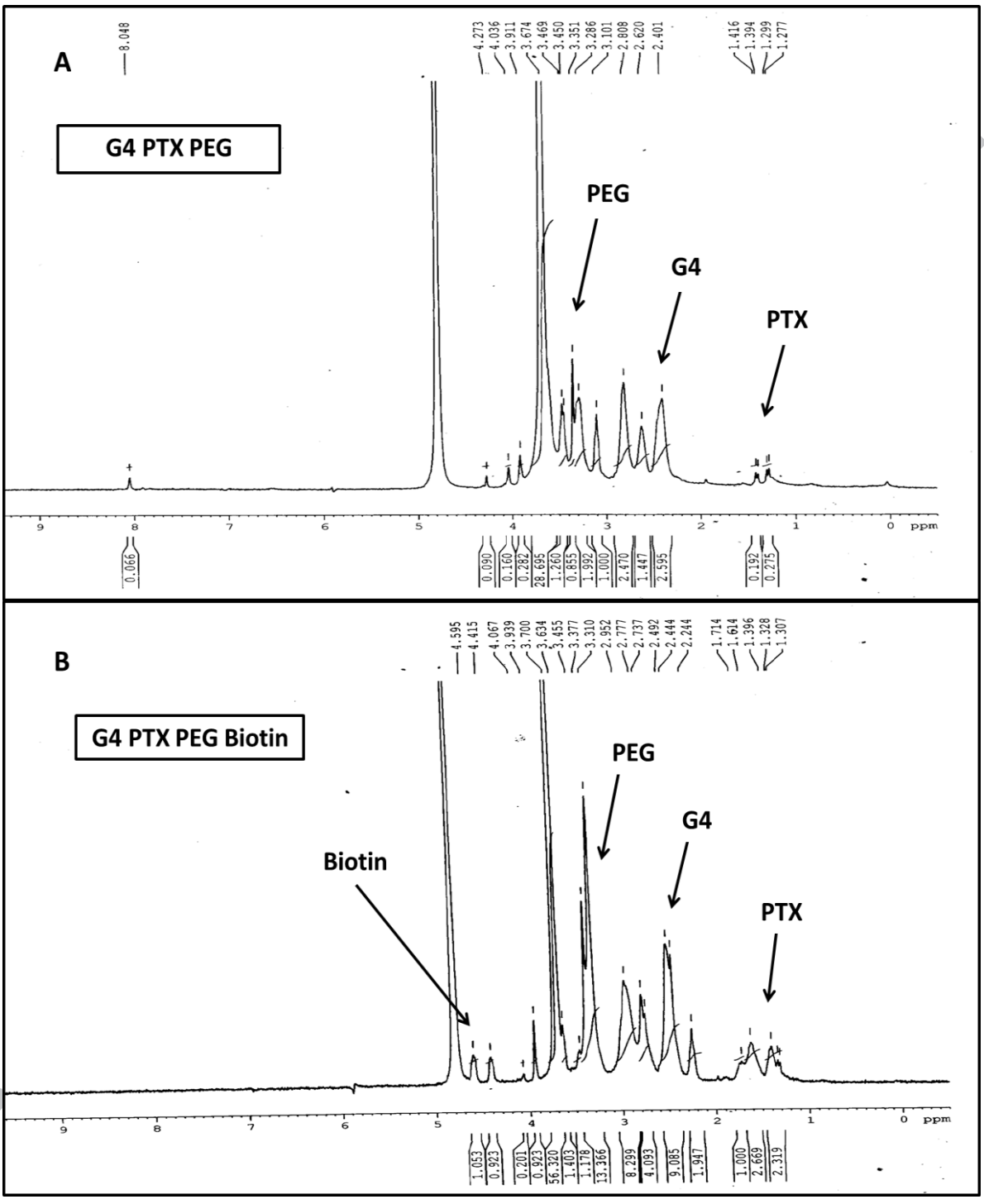

Figure 2C:

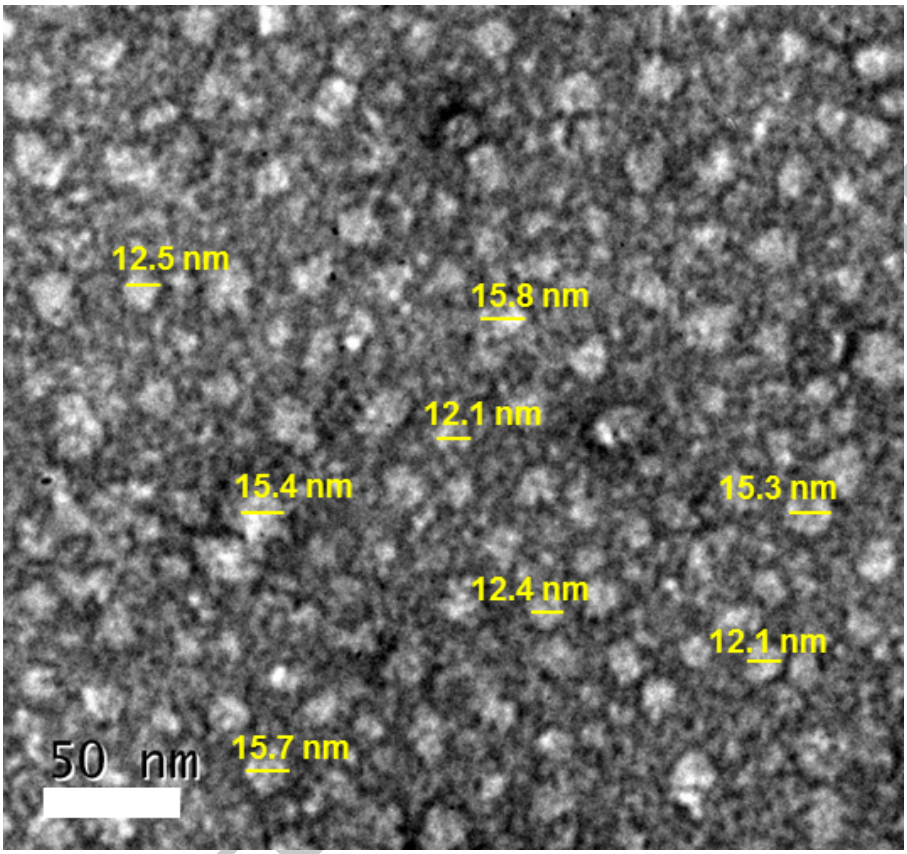

Figure 3:

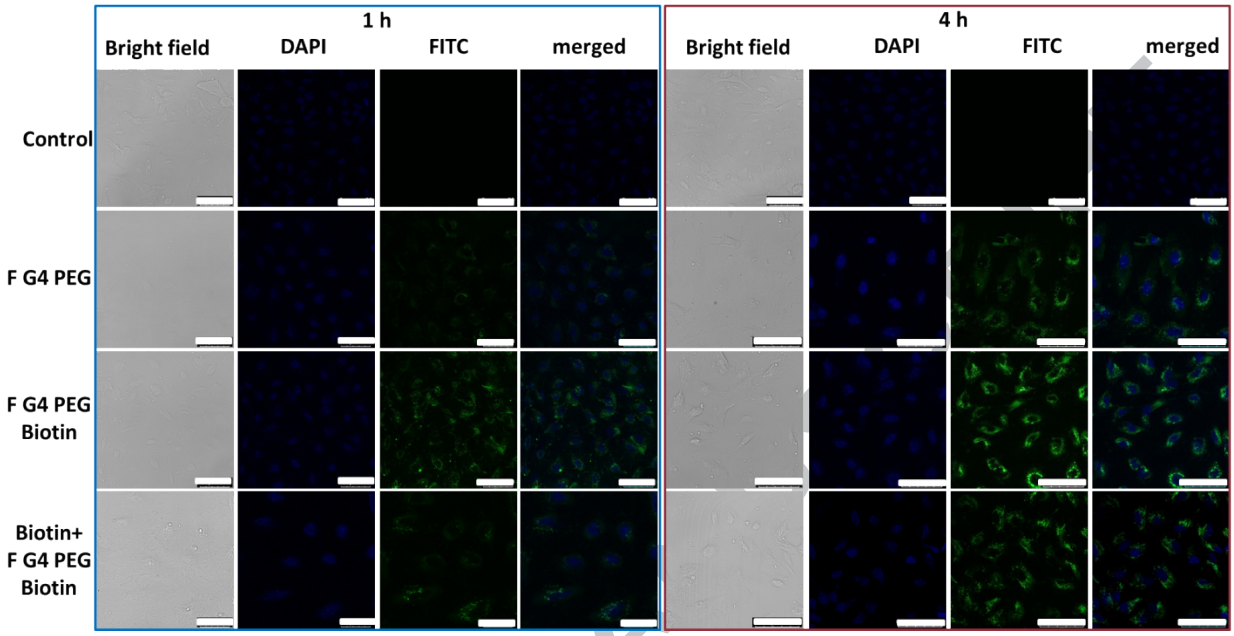

Figure 4:

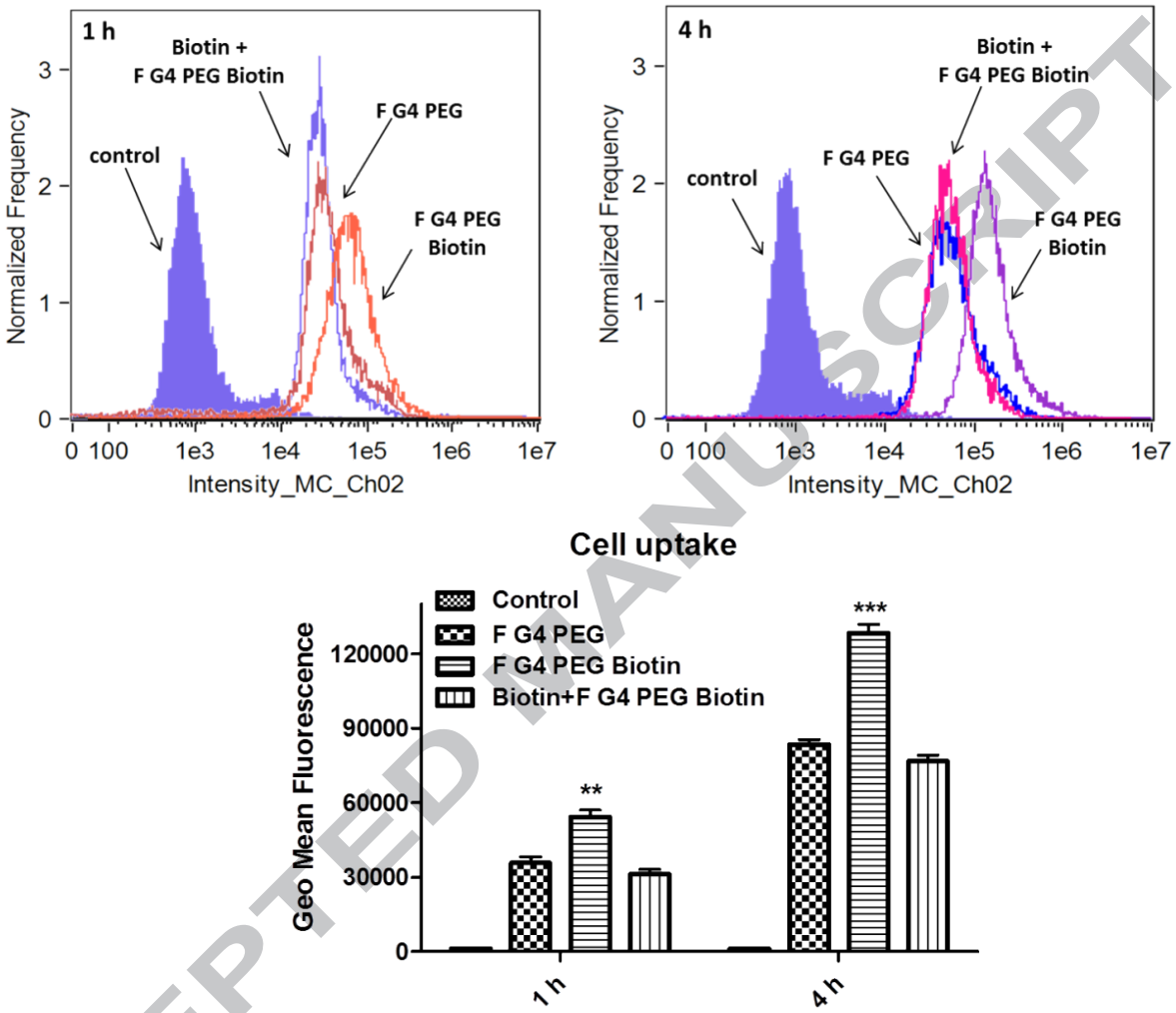

Figure 5:

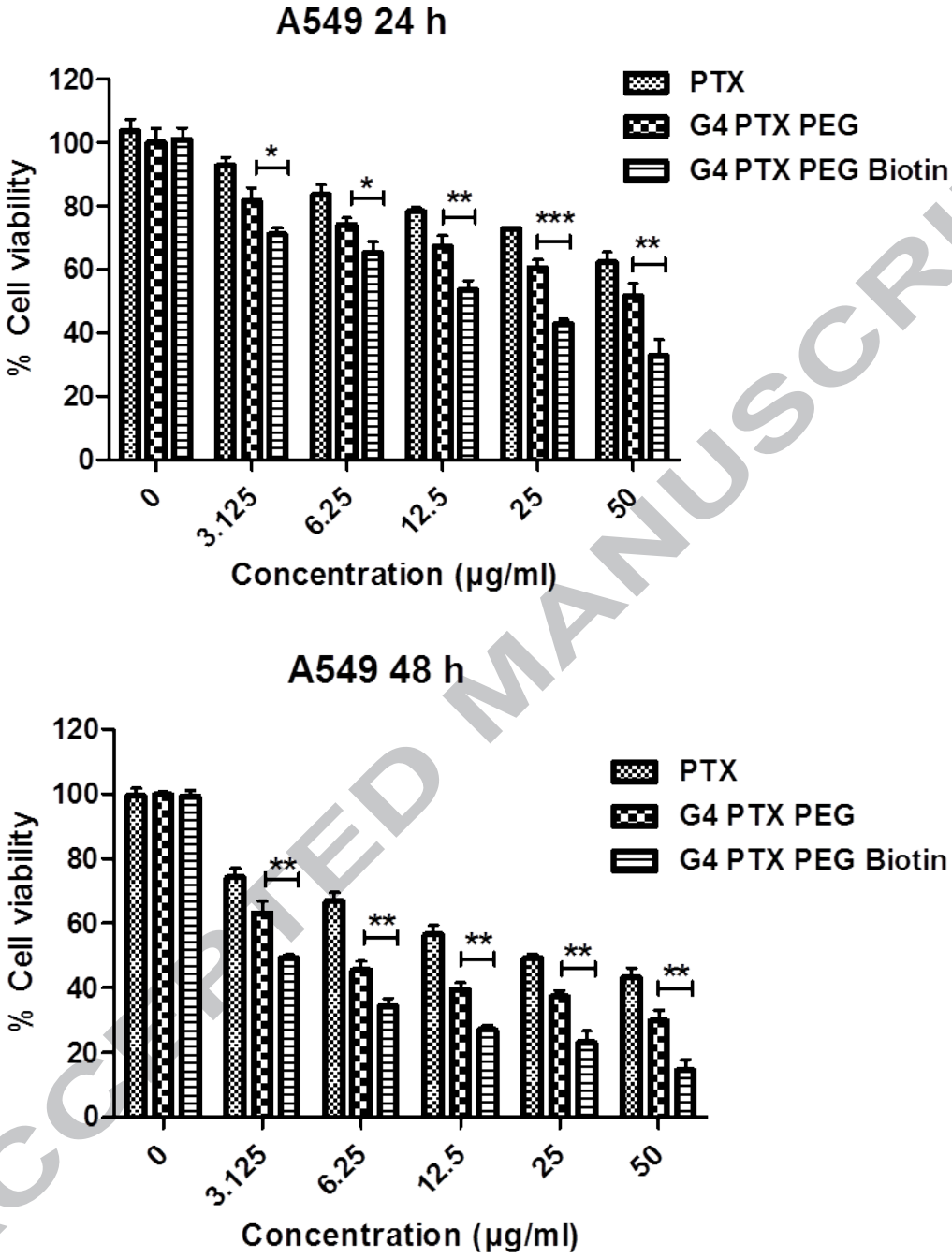

Figure 6:

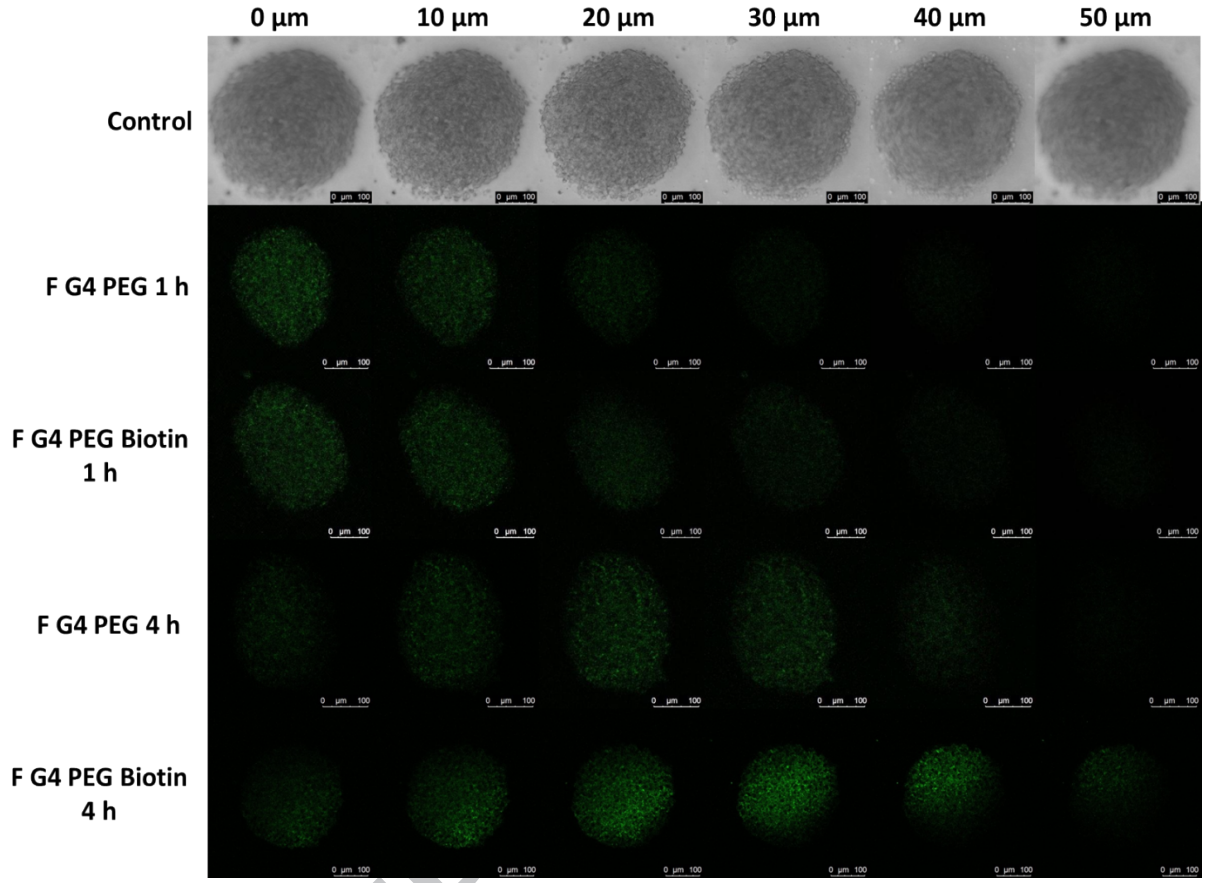

Figure 7:

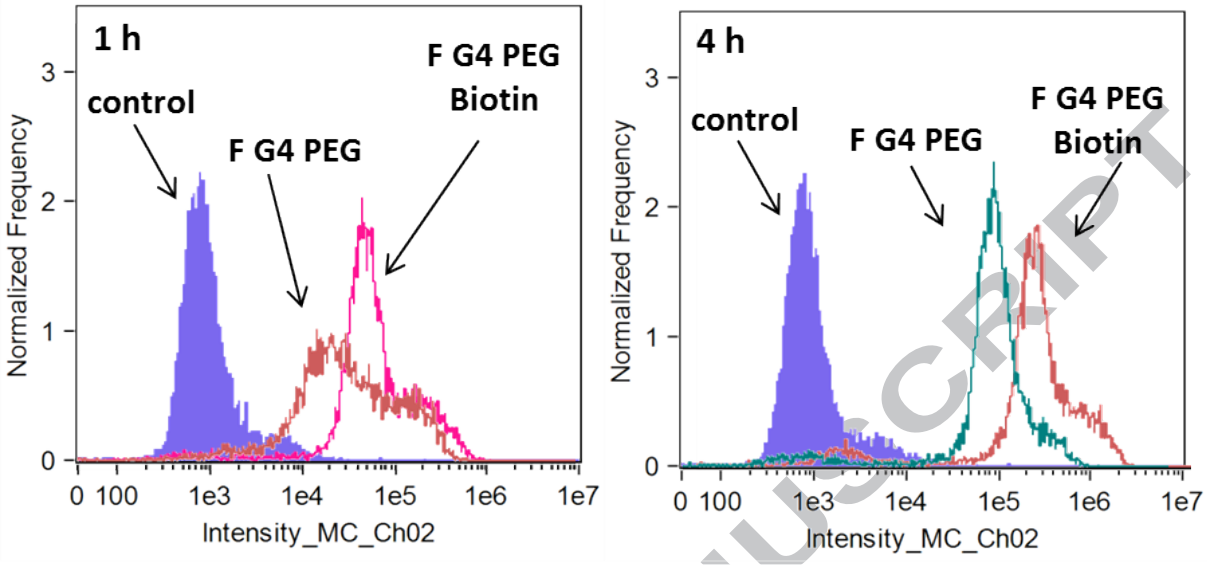
1 h
control
F G4 PEG
F G4 PEG Biotin
Normalized Frequency
Intensity_MC_Ch02
4 h
control
F G4 PEG
F G4 PEG Biotin
Normalized Frequency
Intensity_MC_Ch02

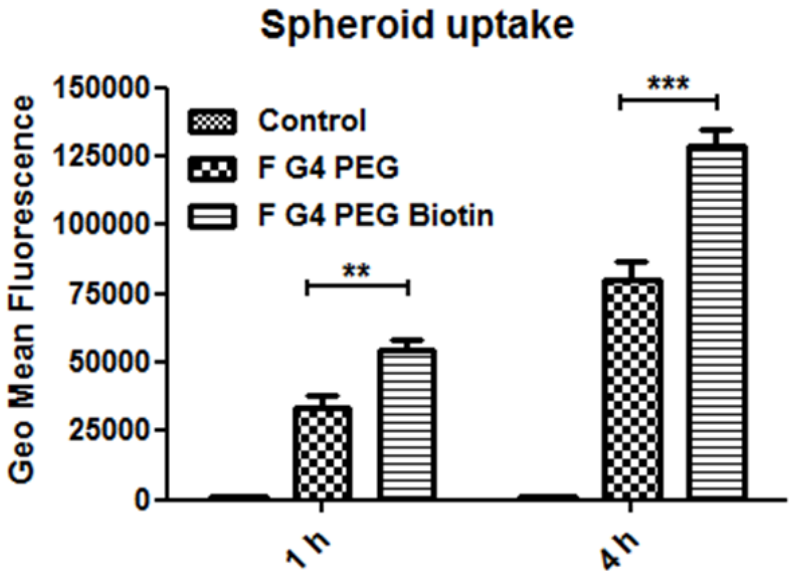
Spheroid uptake
Geo Mean Fluorescence
Control
F G4 PEG
F G4 PEG Biotin
**
***
1 h
4 h

Figure 8:

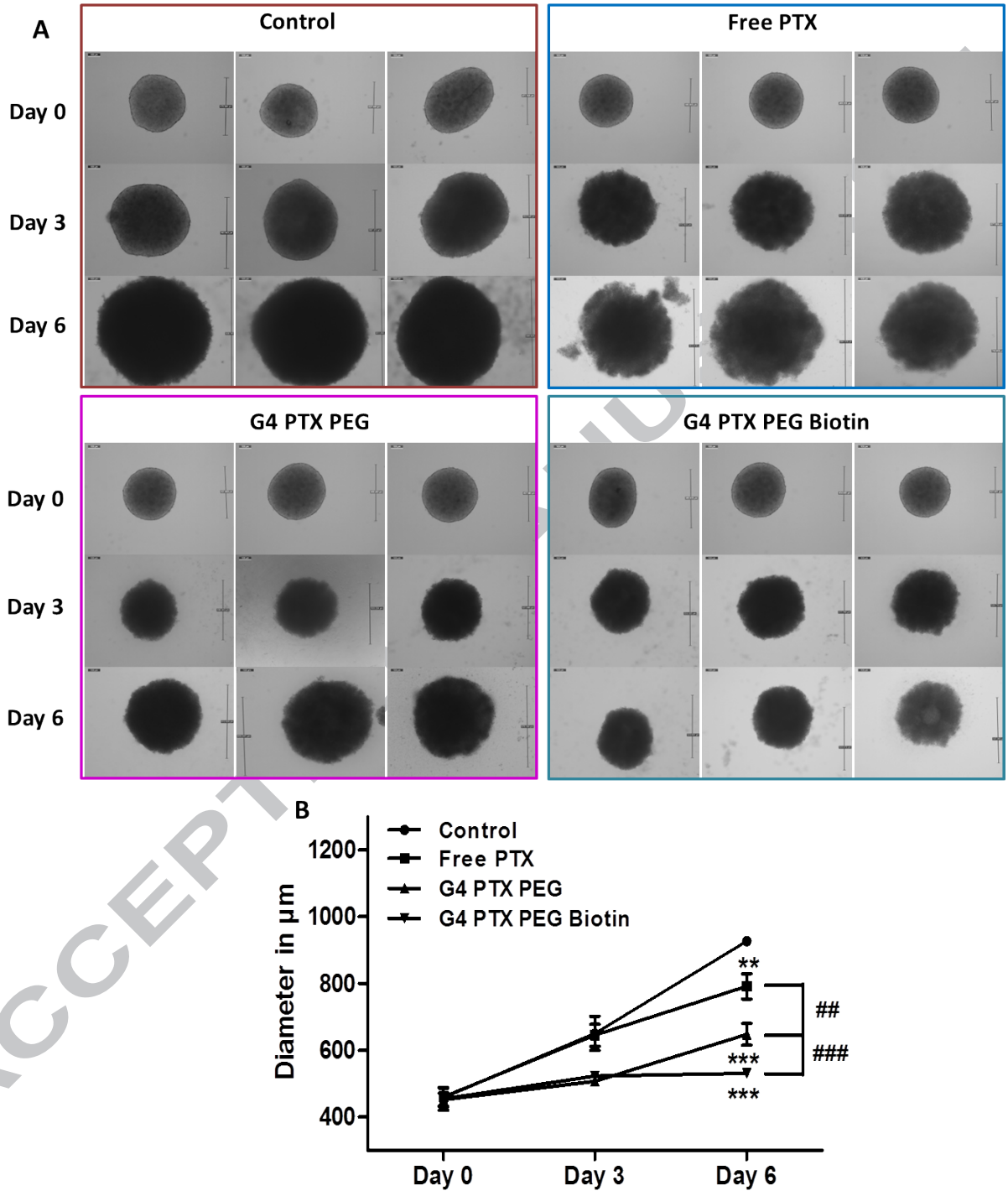

Figure 9:

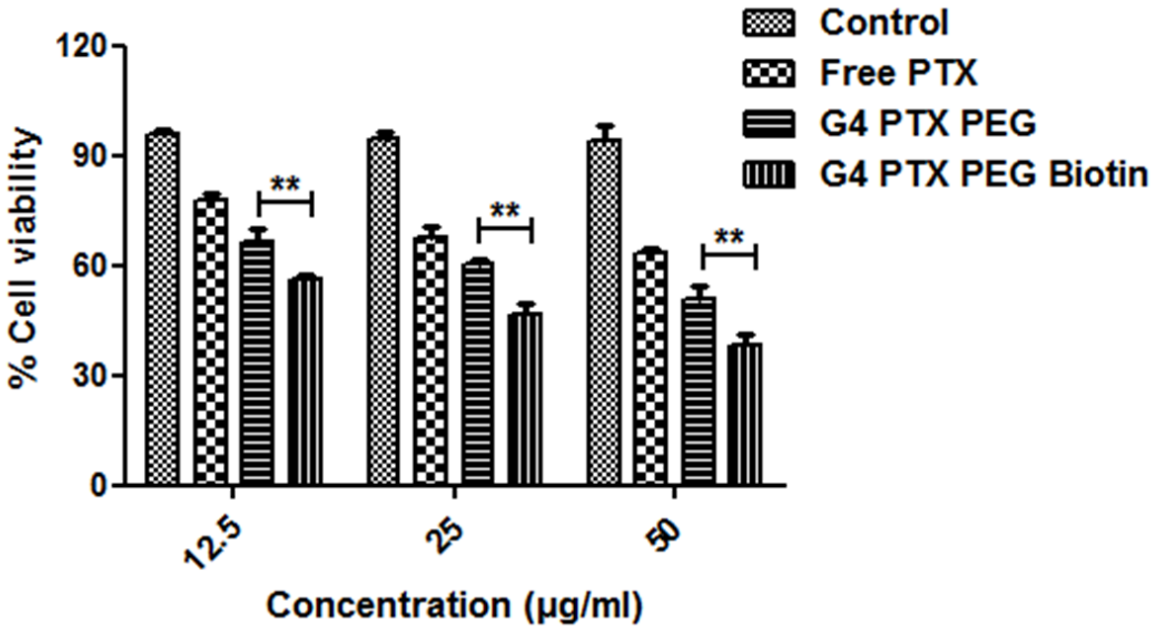

Figure 10:

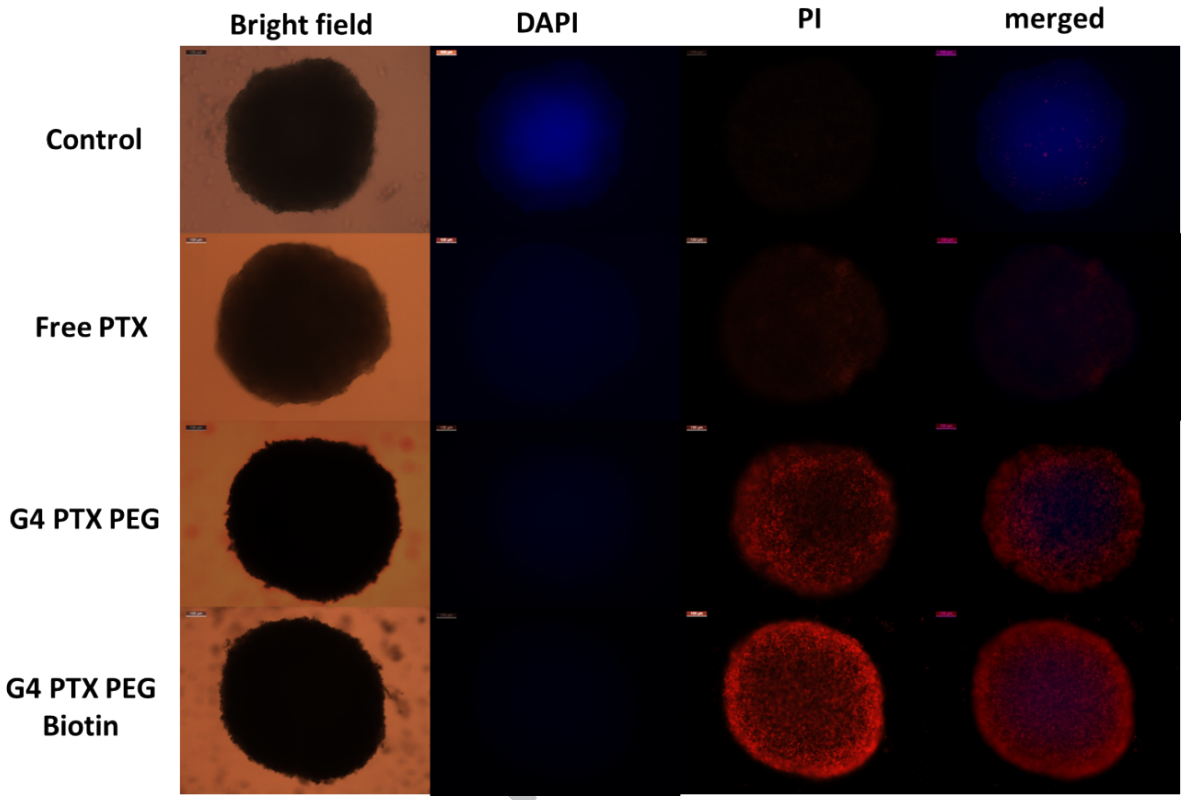

Graphical Abstract

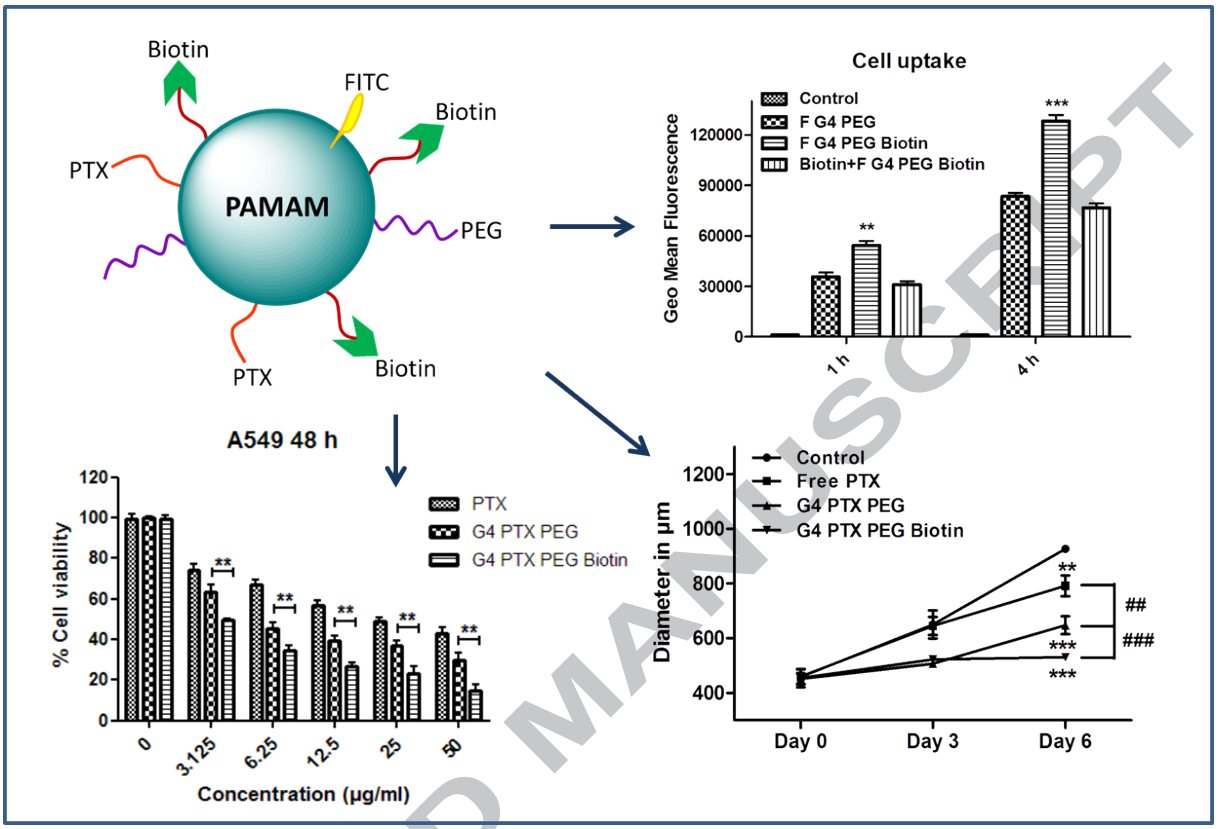

Declaration of interests

☒ The authors declare that they have no known competing financial interests or personal relationships that could have appeared to influence the work reported in this paper.

☐The authors declare the following financial interests/personal relationships which may be considered as potential competing interests: